Acta Neuropathol (2013) 126:711–724
DOI 10.1007/s00401-013-1183-9

ORIGINAL PAPER

Astrocytic A20 ameliorates experimental autoimmune encephalomyelitis by inhibiting NF-κB- and STAT1-dependent chemokine production in astrocytes

Xu Wang · Martina Deckert · Nguyen Thi Xuan · Gopala Nishanth · Sissy Just · Ari Waisman · Michael Naumann · Dirk Schlüter

Received: 11 June 2013 / Revised: 20 September 2013 / Accepted: 21 September 2013 / Published online: 29 September 2013

Abstract Single-nucleotide polymorphisms in the tumor necrosis factor, alpha-induced protein 3 gene, which encodes the ubiquitin-modifying protein A20, are linked to susceptibility to multiple sclerosis (MS), a demyelinating autoimmune disease of the central nervous system (CNS). Since it is unresolved how A20 regulates MS pathogenesis, we examined its function in a murine model of MS, namely experimental autoimmune encephalomyelitis (EAE). Deletion of A20 in neuroectodermal cells (astrocytes, neurons, and oligodendrocytes; Nestin-Cre $A20^{fl/fl}$ mice) or selectively in astrocytes (GFAP-Cre $A20^{fl/fl}$ mice) resulted in more severe EAE as compared to control animals. In Nestin-Cre $A20^{fl/fl}$ and GFAP-Cre $A20^{fl/fl}$ mice demyelination and recruitment of inflammatory leukocytes were increased as compared to $A20^{fl/fl}$ control mice. Importantly, numbers of encephalitogenic $CD4^+$ T cells producing interferon (IFN)-γ, interleukin (IL)-17, and granulocyte–macrophage colony-stimulating factor (GM-CSF), respectively, as well as mRNA production of IFN-γ, IL-17, tumor necrosis factor (TNF), GM-CSF, IL-6, CXCL1, CCL2, and CXCL10 were significantly increased in spinal cords of Nestin-Cre $A20^{fl/fl}$ and GFAP-Cre $A20^{fl/fl}$ mice, respectively. Compared to A20-sufficient astrocytes, A20-deficient astrocytes displayed stronger activation of nuclear factor kappa-light-chain enhancer of activated B cells (NF-κB) in response to TNF, IL-17, and GM-CSF, and of signal transducer and activator of transcription 1 (STAT1) upon IFN-γ stimulation. Due to NF-κB and STAT1 hyperactivation, A20-deficient astrocytes produced significantly more chemokines in response to these key encephalitogenic cytokines of autoimmune $CD4^+$ T cells resulting in an amplification of $CD4^+$ T cell recruitment to the CNS. Thus, astrocytic A20 is an important inhibitor of autoimmune-mediated demyelination in the CNS.

Keywords A20 · Astrocytes · Autoimmunity · EAE

Introduction

Single-nucleotide polymorphisms (SNPs) in or close to the human tumor necrosis factor, alpha-induced protein 3 (TNFAIP3) gene, are associated with several human autoimmune diseases including psoriasis, rheumatoid arthritis, type 1 diabetes, systemic lupus erythematosus (SLE), and multiple sclerosis [10, 15, 22, 39, 40, 42], suggesting that altered expression and activity of A20, which is encoded

Electronic supplementary material The online version of this article (doi:10.1007/s00401-013-1183-9) contains supplementary material, which is available to authorized users.

X. Wang · N. T. Xuan · G. Nishanth · S. Just · D. Schlüter (✉)
Institute of Medical Microbiology, Otto-von-Guericke University Magdeburg, Leipzigerstrasse 44, 39120 Magdeburg, Saxony-Anhalt, Germany
e-mail: dirk.schlueter@med.ovgu.de

M. Deckert
Department of Neuropathology, University Hospital Cologne, 50931 Cologne, Germany

A. Waisman
Institute for Molecular Medicine, University Medical Center of the Johannes-Gutenberg University of Mainz, 55131 Mainz, Germany

M. Naumann
Institute of Experimental Internal Medicine, Otto-von-Guericke University Magdeburg, 39120 Magdeburg, Germany

D. Schlüter
Helmholtz Centre for Infection Research, 38124 Braunschweig, Germany

by TNFAIP3, contribute to specific autoimmune diseases. A20, a ubiquitin-modifying protein, inhibits activation of nuclear factor kappa-light-chain enhancer of activated B cells (NF-κB) by deubiquitinating K63-linked ubiquitination events and targets proteins, such as receptor-interacting protein 1 (RIP1), for proteasomal degradation by adding K48-linked polyubiquitin chains [33, 46, 57]. Experimental studies in mice have elucidated B cell-, dendritic cell-, and myeloid cell-specific functions of A20 in the development of autoimmunity [8, 18, 21, 25, 34, 50]. However, it is still unclear whether A20 expression in non-hematogenous organ-resident cells contributes to the regulation of autoimmune diseases including multiple sclerosis (MS) and its murine model experimental autoimmune encephalomyelitis (EAE).

EAE can be actively induced in mice by immunization with central nervous system (CNS) autoantigens resulting in the induction of autoimmune $CD4^+$ T cells, which are subsequently recruited to the CNS and initiate demyelination [3, 35]. Among $CD4^+$ T lymphocytes, T helper 1 (Th1), T helper 17 (Th17), and granulocyte–macrophage colony-stimulating factor (GM-CSF)-producing $CD4^+$ T cells have been identified as important mediators in the immunopathogenesis of EAE and all of them can induce EAE independently [9, 12, 26, 29, 49].

To some extent, T cell responses can be regulated by CNS-resident cells; therefore, several CNS-resident cell populations are also involved in the regulation of EAE. Neurons, though often neglected as immune-regulating cells, contribute to the suppression of EAE by mediating the conversion of encephalitogenic T cells to $CD25^+$ $Foxp3^+$ regulatory T cells [31]. As active players in CNS innate immunity, astrocytes play both beneficial and detrimental roles in EAE [38, 41, 48, 56]. We have shown before that glycoprotein 130 (gp130)-dependent astrocyte survival and astrogliosis are critical to restrict CNS inflammation during EAE [20]. We also found that, in the recovery stage of EAE, astrocytic Fas ligand contributed to the apoptotic elimination of encephalitogenic $CD4^+$ T cells from the CNS, thereby determining recovery from EAE [56]. As an important source of proinflammatory cytokines and chemokines, astrocytes contribute to EAE pathogenesis by regulating the recruitment of inflammatory cells [38, 41]. Noteworthy, the NF-κB signaling cascade plays a pivotal role in astrocytic chemokine production, and inhibition of NF-κB in astrocytes by deletion of nuclear factor of kappa-light-polypeptide gene enhancer in B-cells inhibitor, alpha (IκBα), inhibitor of nuclear factor kappa-B kinase subunit beta (IKK2), NF-κB essential modulator (NEMO), and Act1, respectively, ameliorates EAE [4, 23, 52].

To address the function of A20 in neuroectodermal cells (astrocytes, neurons, oligodendrocytes) in EAE, we generated Nestin-Cre $A20^{fl/fl}$ mice with specific A20 ablation in neuroectodermal cells and challenged them with EAE. Nestin-Cre $A20^{fl/fl}$ mice developed significantly more severe EAE than control littermates. Furthermore, we identified that astrocytic A20 was responsible for ameliorating EAE by suppressing NF-κB and signal transducer and activator of transcription 1 (STAT1)-dependent chemokine production, and subsequent recruitment of autoimmune $CD4^+$ T cells to the CNS.

Materials and methods

Mice

Nestin-$Cre^{+/-}$ $A20^{fl/fl}$, glial fibrillary acidic protein (GFAP)-$Cre^{+/-}$ $A20^{fl/fl}$, and Synapsin-$Cre^{+/-}$ $A20^{fl/fl}$ mice were generated by crossing C57BL/6 Nestin-Cre [51], GFAP-Cre [2], and Synapsin-Cre [60] mice, respectively, with C57BL/6 $A20^{fl/fl}$ [21] mice. Genotyping of offsprings was carried out by PCR of tail DNA with primers targeting Nestin-Cre, GFAP-Cre, Synapsin-Cre, and $A20^{fl/fl}$, respectively. C57BL/6 WT mice were obtained from Harlan (Borchen, Germany). Animal care and experimental procedures were performed according to European regulations and approved by state authorities (Landesverwaltungsamt Halle, Germany).

Induction and assessment of EAE

EAE was induced in 8- to 12-week-old mice by subcutaneous immunization with 200 μg of myelin oligodendrocyte glycoprotein $(MOG)_{35–55}$ (MEVGWYRSPFSRVVHLYRNGK) peptide (JPT, Berlin, Germany) emulsified in complete Freund's adjuvant (Sigma) supplemented with 800 μg of killed *Mycobacterium tuberculosis* (Sigma). In addition, 200 ng pertussis toxin (Sigma) in 200 μl PBS was administered intraperitoneally on day 0 and day 2 post immunization (p.i.). Clinical signs of EAE were monitored and scored daily according to a scale of severity from 0 to 5 as described previously [56]. Daily clinical scores were calculated as the average of all individual disease scores within each group.

Isolation of intraspinal leukocytes and flow cytometry

Leukocytes were isolated from the spinal cord and stained for CD4, CD8, and CD45 as described before [56]. For the detection of cytokine-producing $CD4^+$ T cells, isolated leukocytes were incubated with 50 ng/ml PMA, 500 ng/ml ionomycin, Golgi-Plug (1 μl/ml) containing brefeldin A in RPMI-1640 at 37 °C for 4 h. Thereafter, cells were stained with rat anti-mouse CD4-FITC, rat

anti-mouse CD45-V450, fixed and permeabilized with Cytofix/Cytoperm (BD), and stained with rat anti-mouse interleukin 17 (IL-17)-PE, interferon gamma (IFN-γ)-PE, and GM-CSF-PE, respectively. All antibodies were purchased from BD. Flow cytometry was performed on a FACSCantoII (BD).

Cell culture

Primary astrocytes were isolated from 1- to 2-day-old newborn mice and cultured as published before [19]. To eliminate microglia from astrocyte cultures, cells were harvested from astrocyte cultures and stained with rat anti-mouse CD11b-PE. Astrocytes ($CD11b^-$) were then separated from $CD11b^+$ microglia with a FACSVantage cell sorter (BD). Neuronal cultures were obtained as published before [19]. In brief, pregnant female mice were killed by cervical dislocation at gestational day 18.5, and dissociated cells of each embryonic brain were cultivated in flasks coated with poly-D-lysine in Neurobasal medium supplemented with B27 (Invitrogen) and 500 μM L-glutamine (Gibco). The purity of cultures for neurons was >98 %, as determined by immunofluorescence staining for neuron-specific class III β-tubulin.

Histology

For histology on paraffin sections, mice anesthetized with methoxyflurane were perfused with 0.1 M PBS followed by 4 % paraformaldehyde in PBS. Spinal cords were processed and stained with hemalum and eosin and cresyl violet/luxol fast blue. For macrophage and neurofilament staining, spinal cords were stained with rat anti-mouse Mac-3 (BD) and rabbit anti-neurofilament light (NF-L, Chemicon, Limburg, Germany), respectively, in an ABC protocol with 3,3′-diaminobenzidine (Sigma) and H_2O_2 (Merck) as substrate.

RNA interference

Astrocytes were transfected with small interfering RNA (siRNA) targeting A20 or STAT1 (pre-designed siRNA, Applied Biosystems) with the help of Lipofectamine RNAiMAX Reagent (Invitrogen). Sixty hours posttransfection, cells were used for experiments.

Quantitative RT-PCR

Total mRNA was isolated from spinal cord and cultured astrocytes according to the manufacturer's instructions (RNeasy kit, Qiagen). The SuperScript reverse transcriptase kit with oligo (dT) primers (Invitrogen) was used to generate cDNA. Quantitative RT-PCR for A20, IL-17, IFN-γ, interleukin 6 (IL-6), GM-CSF, tumor necrosis factor (TNF), chemokine (C–X–C motif) ligand 1 (CXCL1), chemokine (C–C motif) ligand 2 (CCL2), C–X–C motif chemokine 10 (CXCL10), STAT1, and hypoxanthine phosphoribosyltransferase (HPRT) (Applied Biosystems) was performed on the Lightcycler 480 system (Roche). The ratio between the respective gene and corresponding HPRT was calculated per sample according to the ΔΔ cycle threshold method [32].

Western blotting

Cultured astrocytes, neurons, and microglia were stimulated as indicated and lysed in RIPA1 buffer. Cytoplasmic and nuclear protein fractions were extracted with NE-PER Nuclear and Cytoplasmic Extraction Kit (Thermo Scientific). Lysates were cleared by centrifugation at 14,000*g* for 20 min at 4 °C. Supernatants were harvested, heated in lane marker reducing sample buffer (Thermo Scientific) and run on SDS-PAGE. Immunoblots were probed for A20 (Santa Cruz), histone deacetylases (HDAC) (Santa Cruz), β-Tubulin (Sigma), phospho-IκBα, IκBα, phospho-p38, p38, phospho-ERK, ERK, JNK, phospho-JNK, phospho-STAT1 (701), phospho-STAT1 (727), STAT1, and glyceraldehyde 3-phosphate dehydrogenase (GAPDH) (Cell Signaling).

Migration assay

Medium was collected from astrocyte cultures untreated or stimulated with IFN-γ (10 ng/ml) for 48 h. $CD4^+$ T cells were isolated from lymph nodes of C57BL/6 mice and placed in the upper part of Transwell chambers (Costar) precoated with 0.01 % poly-L-lysine (Sigma). Conditioned astrocyte medium was added to the lower part. After 2 h of incubation at 37 °C, EDTA was added to stop migration and number of $CD4^+$ T cells in the lower chamber was counted microscopically.

Statistics

To test for statistical differences, the two-tailed Student's *t* test was used. p values <0.05 were accepted as significant. All experiments were performed at least twice.

Results

Upregulation of A20 in the spinal cord during EAE

To explore a possible role of A20 in EAE, C57BL/6 mice were actively immunized with $MOG_{35–55}$ peptide and A20 mRNA expression was analyzed by quantitative real-time

PCR in spinal cord at day 15 and day 22 p.i., respectively. A20 mRNA expression was significantly upregulated in the spinal cord at both day 15 and day 22 p.i. (Online Resource 1) suggesting a possible function of CNS-derived A20 during EAE.

Aggravated EAE of Nestin-Cre A20$^{fl/fl}$ mice

To study the contribution of A20 derived from CNS-resident cells to EAE, we generated Nestin-Cre A20$^{fl/fl}$ mice, which lacked A20 specifically in all neuroectodermal cells including astrocytes, neurons, and oligodendrocytes [17]. Western blot (WB) performed on spinal cord tissue samples from Nestin-Cre A20$^{fl/fl}$ mice and control littermates revealed that A20 expression was deleted in spinal cord of Nestin-Cre A20$^{fl/fl}$ mice (Fig. 1a). Similar result was also obtained with quantitative real-time PCR (Fig. 1b). Upon induction of EAE by active immunization with $MOG_{35–55}$ peptide, Nestin-Cre A20$^{fl/fl}$ mice displayed significantly stronger clinical symptoms as compared to the control A20$^{fl/fl}$ mice (Fig. 1c). Noteworthy, the more severe EAE of Nestin-Cre A20$^{fl/fl}$ mice cannot be attributed to the Nestin-Cre transgene, since Nestin-Cre A20$^{wt/wt}$ mice developed the same course of disease as A20$^{wt/wt}$ mice (Online Resource 2). Both A20$^{fl/fl}$ and Nestin-Cre A20$^{fl/fl}$ mice developed EAE with demyelination in the spinal cord, which was, however, more pronounced and widespread in Nestin-Cre A20$^{fl/fl}$ mice at days 15 and 22 p.i. (Fig. 1d, upper panel, cresyl violet/luxol fast blue staining). In addition, macrophage infiltration of the spinal cord was more prominent in Nestin-Cre A20$^{fl/fl}$ mice at days 15 and 22 p.i. (Fig. 1d, middle panel, anti-Mac3 staining). At day 15 p.i., mild axonal damage was visible in both strains of mice (Fig. 1d, lower panel, anti-neurofilament staining). In A20$^{fl/fl}$ mice axonal damage remained mild at day 22 p.i., whereas it progressed in Nestin-Cre A20$^{fl/fl}$ mice (Fig. 1d, lower panel, anti-neurofilament staining).

The percentage and number of infiltrating CD4$^+$ T cells did not differ between unimmunized animals of both mouse strains (day 0) showing that Nestin-Cre A20$^{fl/fl}$ mice did not develop spontaneous inflammation in the CNS (Fig. 1e, f). At day 15 p.i., a higher percentage of CD4$^+$ T cells infiltrating the spinal cord was detected in Nestin-Cre A20$^{fl/fl}$ mice (Fig. 1e). At day 22 p.i., the time point when Nestin-Cre A20$^{fl/fl}$ mice showed significantly more severe clinical symptoms than control mice, the percentage and number of invading CD4$^+$ T cells were significantly higher in the spinal cord of Nestin-Cre A20$^{fl/fl}$ mice (Fig. 1e, f). Correspondingly, at day 22 p.i., higher levels of proinflammatory IFN-γ, IL-17, TNF, GM-CSF, IL-6, CXCL1, CCL2, and CXCL10 mRNA were detected in the spinal cord of Nestin-Cre A20$^{fl/fl}$ mice (Fig. 1g). Noteworthy, in the CNS, astrocytes are a major inducible source of the chemokines CXCL1, CCL2, and CXCL10 [27, 38], implying that the aggravated EAE in Nestin-Cre A20$^{fl/fl}$ mice might be attributed to the deletion of A20 in astrocytes.

Fig. 1 Aggravation of EAE by deletion of A20 in neuroectodermal cells. **a** WB analysis for A20 in the spinal cord of Nestin-Cre A20$^{fl/fl}$ and A20$^{fl/fl}$ control mice. **b** RT-PCR analysis for A20 mRNA expression in the spinal cord of Nestin-Cre A20$^{fl/fl}$ and A20$^{fl/fl}$ control mice ($n = 3$ for both groups). Data show the mean + SEM. **c** Clinical scores of EAE in Nestin-Cre A20$^{fl/fl}$ ($n = 7$) and A20$^{fl/fl}$ ($n = 8$) mice induced by $MOG_{35–55}$-immunization. Data show the mean clinical scores + SEM (*$p < 0.05$). **d** *Upper panel* (cresyl violet/luxol fast blue staining): at day 15 p.i., an inflammatory infiltrate is present in the leptomeninges of the posterior columns (*arrow*) with only mild edema in an A20$^{fl/fl}$ mouse. In a Nestin-Cre A20$^{fl/fl}$ mouse, the dorsal columns of the spinal cord and the overlying leptomeninges are heavily infiltrated by leukocytes (*arrows*); focal loss of myelin and pronounced edema (*stars*) at day 15 p.i. At day 22 p.i, inflammation has regressed in an A20$^{fl/fl}$ mouse with a perivascular infiltrate (*arrow*) in the posterior columns of the spinal cord slightly extending into the adjacent white matter. In a Nestin-Cre A20$^{fl/fl}$ mouse, prominent and poorly demarcated inflammatory infiltrates in the dorsal column extend into the adjacent white matter (*arrows*). Demyelination and edema are severe (*stars*). *Middle panel* (anti-Mac3 staining): at day 15 p.i., Mac3$^+$ macrophages contribute to the infiltrate in the posterior columns in an A20$^{fl/fl}$ mouse (*arrow*). In a Nestin-Cre A20$^{fl//fl}$ mouse macrophages are also present in infiltrates in the posterior dorsal spinocerebellar tract (*arrows*). At day 22 p.i., Mac3$^+$ macrophages are confined to the dorsal column (*arrow*) in an A20$^{fl/fl}$ mouse, whereas macrophage infiltration extends to the white matter in a Nestin-Cre A20$^{fl/fl}$ mouse (*arrows*). *Lower panel* (anti-neurofilament staining): at day 15 p.i., axonal damage with formation of axonal bulbs is mild in an A20$^{fl/fl}$ mouse and a Nestin-Cre A20$^{fl/fl}$ mouse (*arrows*). At day 22 p.i., mild axonal damage is confined to the dorsal column of an A20$^{fl/fl}$ mouse (*arrow*), whereas axonal damage is severe in a Nestin-Cre A20$^{fl/fl}$ mouse as evidenced by multiple axonal bulbs (*arrows*). Original magnification ×200. **e** CD4$^+$ and CD8$^+$ T cells infiltrating the spinal cords of $MOG_{35–55}$-immunized Nestin-Cre A20$^{fl/fl}$ and A20$^{fl/fl}$ mice were analyzed by flow cytometry at day 0, 15 and 22 p.i. *Representative dot plots* are shown. **f** Absolute number of CD4$^+$ and CD8$^+$ T cells in the spinal cords of $MOG_{35–55}$-immunized Nestin-Cre A20$^{fl/fl}$ and A20$^{fl/fl}$ mice at day 0 ($n = 4$ for both groups) and 22 p.i. ($n = 6$ for both groups) (mean + SEM *$p < 0.05$). **g** RT-PCR analysis of relative expression of inflammatory genes as indicated in spinal cords of $MOG_{35–55}$-immunized Nestin-Cre A20$^{fl/fl}$ and A20$^{fl/fl}$ mice ($n = 3$ for both groups) at day 22 p.i. Data represent the mean + SEM as relative increase over unimmunized mice

A20 deficiency in astrocytes but not in neurons aggravates EAE

In order to precisely elucidate the function of astrocytic A20 in EAE, we generated GFAP-Cre A20$^{fl/fl}$ mice, in which A20 was selectively ablated in astrocytes, and explored their susceptibility to EAE. A20 deletion was detected in astrocytes (Fig. 2a), but not in other brain-resident cells including microglia and neurons (Online Resource 3a), though it has been shown that low levels of gene deletion can occur in neurons of GFAP-Cre expressing

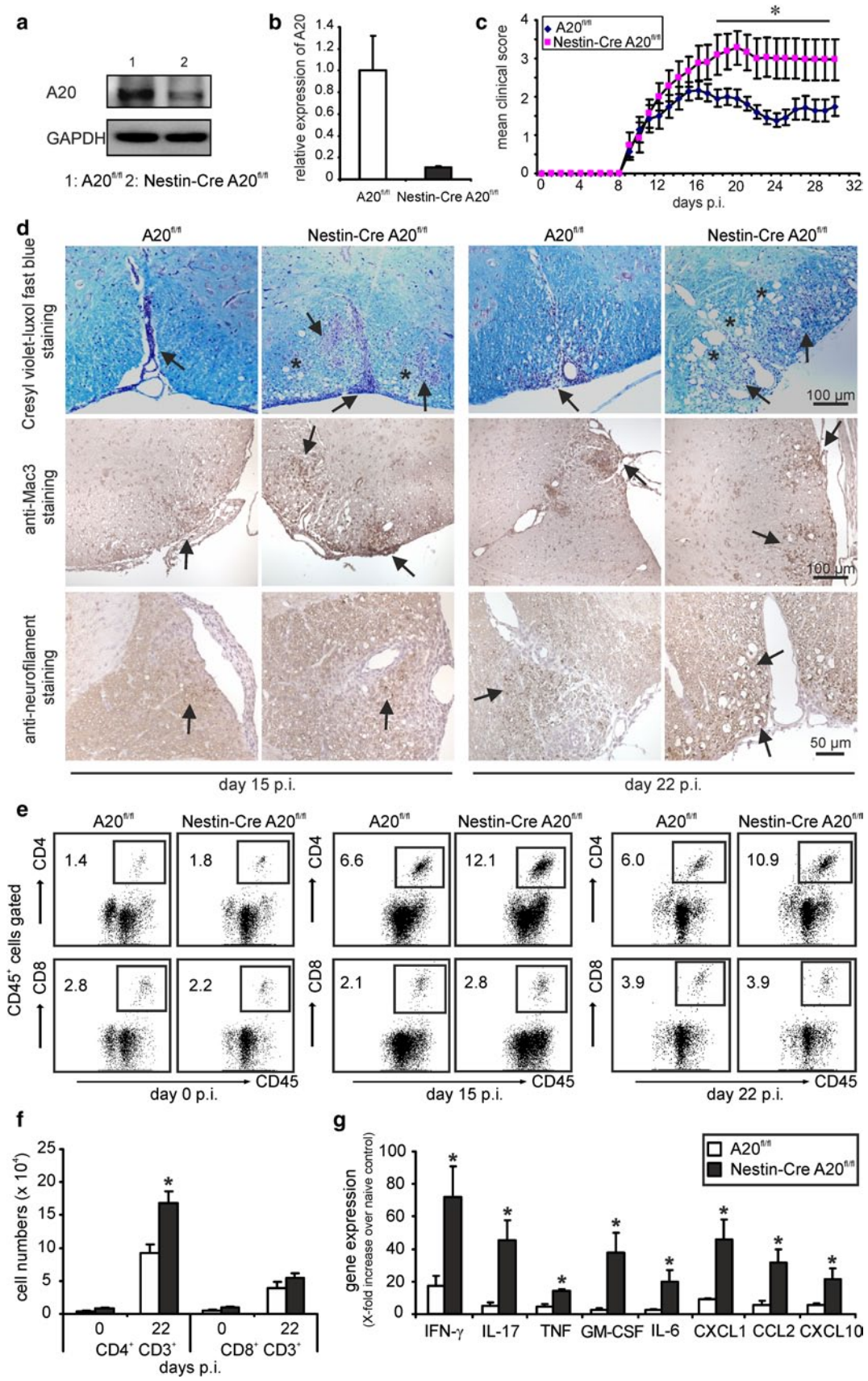
a
1
2
A20
GAPDH
1: A20fl/fl 2: Nestin-Cre A20fl/fl
b
relative expression of A20
1.4
1.2
1.0
0.8
0.6
0.4
0.2
0
A20fl/fl
Nestin-Cre A20fl/fl
c
A20fl/fl
Nestin-Cre A20fl/fl
mean clinical score
*
0
4
8
12
16
20
24
28
32
days p.i.
d
A20fl/fl
Nestin-Cre A20fl/fl
A20fl/fl
Nestin-Cre A20fl/fl
Cresyl violet-luxol fast blue staining
anti-Mac3 staining
anti-neurofilament staining
100 µm
100 µm
50 µm
day 15 p.i.
day 22 p.i.
e
A20fl/fl
Nestin-Cre A20fl/fl
A20fl/fl
Nestin-Cre A20fl/fl
A20fl/fl
Nestin-Cre A20fl/fl
CD45+ cells gated
CD4
CD8
1.4
1.8
2.8
2.2
6.6
12.1
2.1
2.8
6.0
10.9
3.9
3.9
CD45
day 0 p.i.
day 15 p.i.
day 22 p.i.
f
cell numbers (x 10⁴)
25
20
15
10
5
0
*
0
22
0
22
CD4+ CD3+
CD8+ CD3+
days p.i.
g
A20fl/fl
Nestin-Cre A20fl/fl
gene expression
(X-fold increase over naive control)
100
80
60
40
20
0
IFN-γ
IL-17
TNF
GM-CSF
IL-6
CXCL1
CCL2
CXCL10

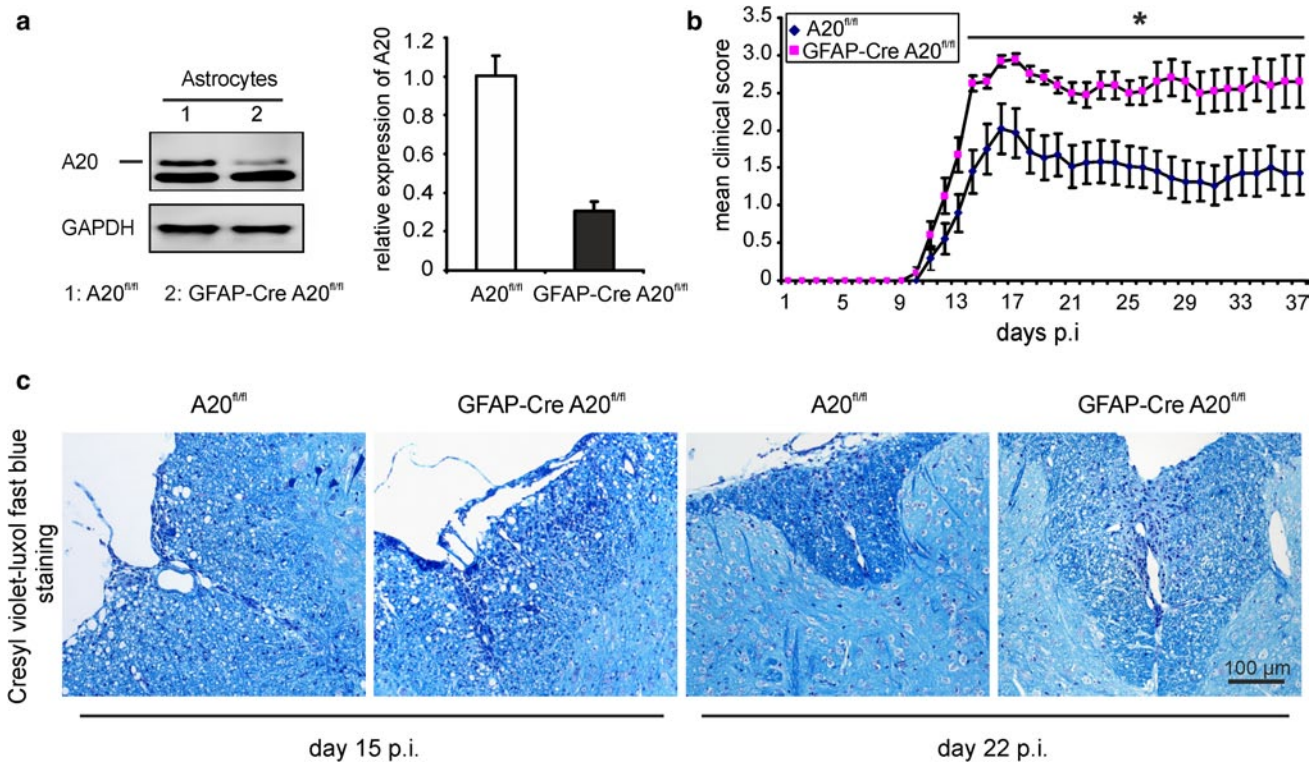

Fig. 2 Aggravation of EAE by ablation of A20 in astrocytes. **a** WB analysis for A20 expression in cultured astrocytes isolated from GFAP-Cre $A20^{fl/fl}$ and $A20^{fl/fl}$ control mice (*left*). The *right panel* shows the relative quantification of A20 normalized to GAPDH. Data show the mean + SEM. **b** Clinical scores of EAE in GFAP-Cre $A20^{fl/fl}$ ($n = 10$) and $A20^{fl/fl}$ ($n = 15$) mice induced by $MOG_{35–55}$ immunization. Data show the mean clinical scores + SEM ($^*p < 0.05$). **c** At day 15 p.i., a GFAP-Cre $A20^{fl/fl}$ mouse shows widespread inflammation, edema, and focal loss of myelin in the posterior columns and the spinocerebellar tracts. In contrast, inflammation and demyelination are much milder in an $A20^{fl/fl}$ mouse. At day 22 p.i., inflammation and demyelination are still active in the posterior columns of a GFAP-Cre $A20^{fl/fl}$ mouse, whereas they have declined in an $A20^{fl/fl}$ mouse. Cresyl violet/luxol fast blue staining. Original magnification ×200

mice. Similar to Nestin-Cre $A20^{fl/fl}$ mice, GFAP-Cre $A20^{fl/fl}$ mice showed significantly more severe clinical symptoms than control mice after EAE induction by $MOG_{35–55}$ immunization (Fig. 2b), demonstrating that A20 in astrocytes is important for the amelioration of EAE. Histology showed that GFAP-Cre $A20^{fl/fl}$ mice displayed more pronounced demyelination in the spinal cord than control mice at day 15 p.i. (Fig. 2c). Up to day 22 p.i., demyelination had regressed in $A20^{fl/fl}$ mice, but persisted in GFAP-Cre $A20^{fl/fl}$ mice. EAE symptoms of GFAP-Cre $A20^{wt/wt}$ mice were similar to that of $A20^{wt/wt}$ mice (Online Resource 3b) ruling out the possibility that the more severe EAE of GFAP-Cre $A20^{fl/fl}$ mice was due to the GFAP-Cre transgene. To consolidate the contention that EAE development was not influenced by A20 deletion in neurons, we generated Synapsin-Cre $A20^{fl/fl}$ mice, in which A20 was efficiently and specifically deleted in neurons (Online Resource 3c). Synapsin-Cre $A20^{fl/fl}$ mice developed comparable clinical symptoms as $A20^{fl/fl}$ mice (Online Resource 3d) illustrating that neuronal A20 deletion does not cause aggravation of EAE.

Increased infiltration of inflammatory cells in the spinal cord of GFAP-Cre $A20^{fl/fl}$ mice

In accordance with the histopathological results, the number of leukocytes infiltrating the spinal cord of GFAP-Cre $A20^{fl/fl}$ was increased with a higher percentage of $CD4^+$ T lymphocytes at both early (day 15 p.i.) and late (day 22 p.i) stages of EAE (Fig. 3a, b). The number of infiltrating leukocytes and the percentage of infiltrating $CD4^+$ T cells did not differ between unimmunized animals of both mouse strains (day 0) showing that GFAP-Cre $A20^{fl/fl}$ mice did not develop spontaneous inflammation in the CNS (Fig. 3a, b). In addition to $CD4^+$ T cells, absolute numbers of infiltrating $CD8^+$ T cells, $Ly6C^{hi}$ $CD11b^+$ inflammatory monocytes, and $F4/80^+$ $CD68^+$ macrophages were also significantly increased in the spinal cord of GFAP-Cre $A20^{fl/fl}$ mice at both day 15 and 22 p.i. (Fig. 3c). Given that GM-CSF, IL-17, and IFN-γ-producing T cells can all induce EAE [6, 9, 12] while regulatory $Foxp3^+$ $CD4^+$ T cells suppress the disease [1, 36], we studied these subpopulations of invading $CD4^+$ T cells. At both days 15 and 22 p.i., numbers of

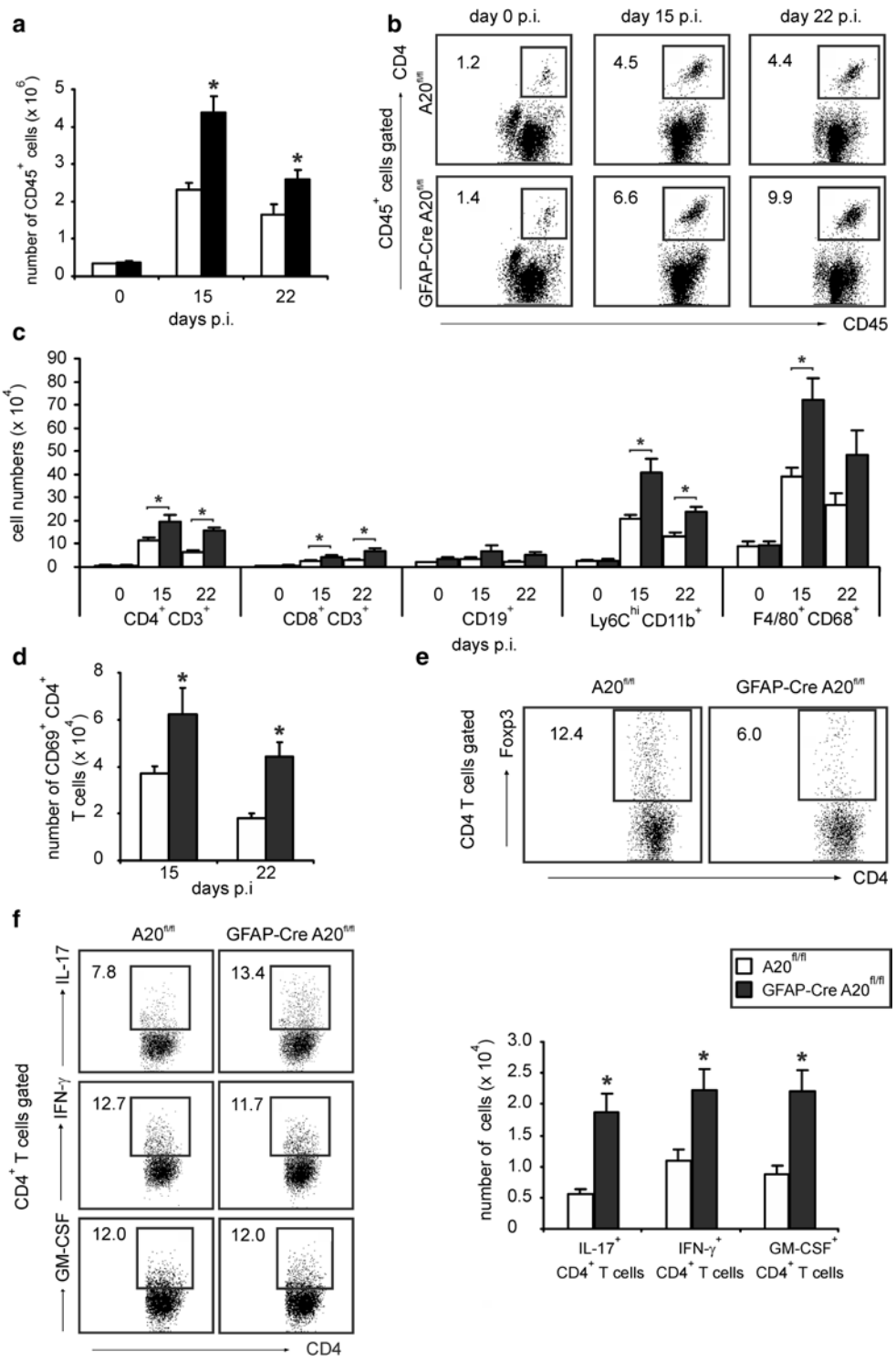

Fig. 3 Increased immune cell infiltration in the spinal cords of GFAP-Cre A20$^{fl/fl}$ mice during EAE. **a** Absolute number of infiltrating CD45$^+$ cells in the spinal cords of unimmunized or $MOG_{35–55}$-immunized GFAP-Cre A20$^{fl/fl}$ and A20$^{fl/fl}$ mice ($n = 6$ for both groups) (mean + SEM $^*p < 0.05$). **b** Percentage of infiltrating CD4$^+$ T cells in the spinal cords of $MOG_{35–55}$-immunized GFAP-Cre A20$^{fl/fl}$ and A20$^{fl/fl}$ mice was analyzed by flow cytometry. *Representative dot plots* are shown. **c** Absolute number of infiltrating immune cells in the spinal cords of GFAP-Cre A20$^{fl/fl}$ and A20$^{fl/fl}$ mice at day 0 ($n = 6$ for both groups), 15 ($n = 6$ for GFAP-Cre A20$^{fl/fl}$ group; $n = 5$ for A20$^{fl/fl}$ group), and 22 ($n = 6$ for both groups) p.i. (mean + SEM $^*p < 0.05$). **d** Absolute number of CD69$^+$ CD4$^+$ T cells was calculated based on flow cytometry results at day 15 ($n = 6$ for GFAP-Cre A20$^{fl/fl}$ group; $n = 5$ for A20$^{fl/fl}$ group) and 22 ($n = 6$ for both groups) p.i. (mean + SEM $^*p < 0.05$). **e** *Representative dot plots* show Foxp3$^+$ CD4$^+$ T cells in the spinal cords of $MOG_{35–55}$-immunized GFAP-Cre A20$^{fl/fl}$ and A20$^{fl/fl}$ mice at day 22 p.i. **f** The relative (*left panel*) and absolute (*right panel*) number of IL-17$^+$ CD4$^+$, IFN-γ$^+$ CD4$^+$, and GM-CSF$^+$ CD4$^+$ T cells in the spinal cords of $MOG_{35–55}$-immunized GFAP-Cre A20$^{fl/fl}$ and A20$^{fl/fl}$ mice ($n = 6$ for both groups) at day 22 p.i. was analyzed by flow cytometry (mean + SEM $^*p < 0.05$)

activated CD69$^+$ CD4$^+$ T cells were increased in the spinal cord of GFAP-Cre A20$^{fl/fl}$ mice (Fig. 3d). In contrast, the percentage of Foxp3$^+$ regulatory CD4$^+$ T cells was significantly decreased in the spinal cord of GFAP-Cre A20$^{fl/fl}$ mice at day 22 p.i. (Fig. 3e). Flow cytometry showed that only the percentage of IL-17 but not of IFN-γ and GM-CSF producing CD4$^+$ T cells was increased in GFAP-Cre A20$^{fl/fl}$ mice. However, the total number of all three T cell populations was significantly increased in the spinal cord of GFAP-Cre A20$^{fl/fl}$ mice as compared to A20$^{fl/fl}$

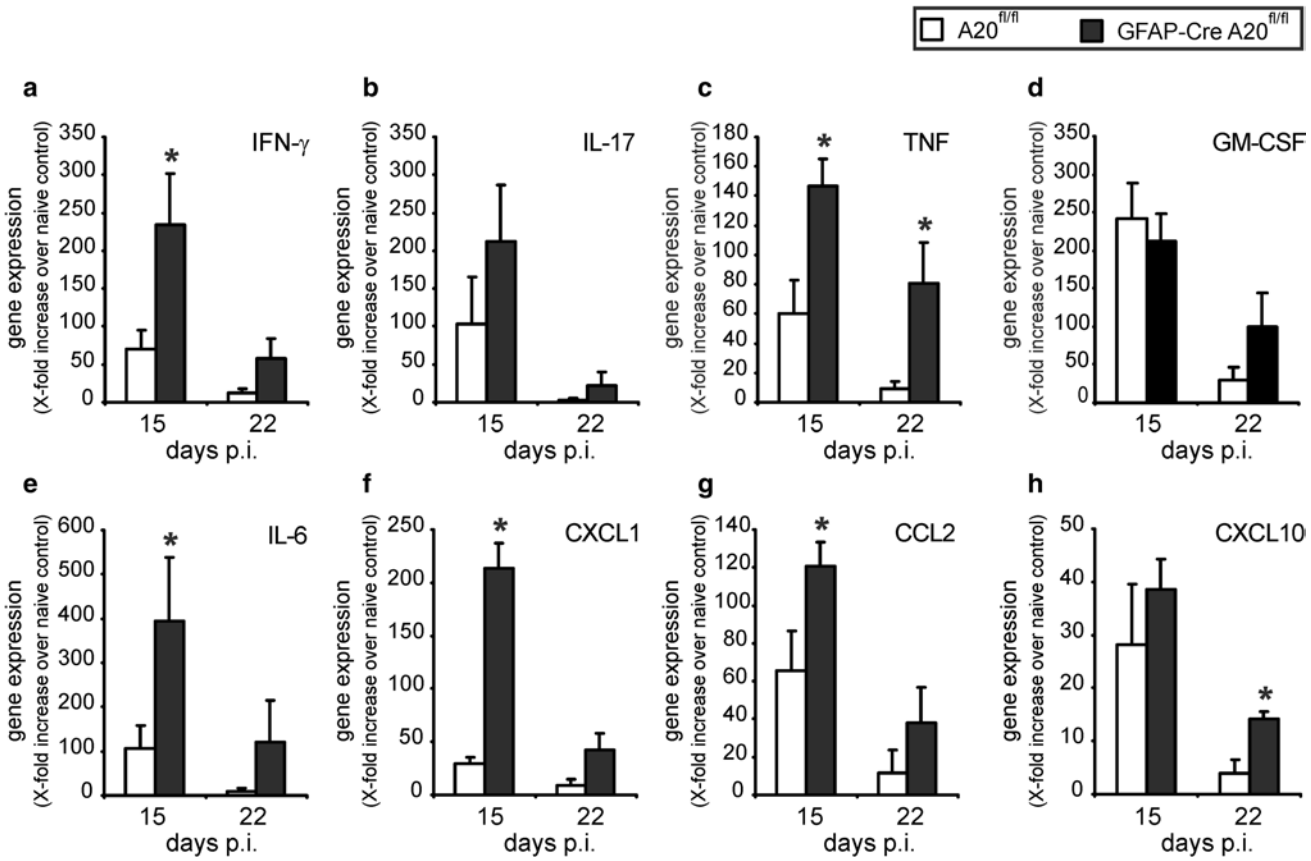

Fig. 4 Increased pro-inflammatory gene expression in the spinal cords of GFAP-Cre A20$^{fl/fl}$ mice. Expression of **a** IFN-γ, **b** IL-17, **c** TNF, **d** GM-CSF, **e** IL-6, **f** CXCL1, **g** CCL2, and **h** CXCL10 mRNA was determined by quantitative RT-PCR in GFAP-Cre A20$^{fl/fl}$ and A20$^{fl/fl}$ mice at days 15 and 22 p.i. Spinal cords of three mice per group were analyzed. Data represent the mean + SEM as relative increase over unimmunized mice (*$p < 0.05$)

mice (Fig. 3f) explaining the more severe EAE in GFAP-Cre A20$^{fl/fl}$ mice.

Increased proinflammatory gene transcription in the spinal cord of GFAP-Cre A20$^{fl/fl}$ mice

To examine the impact of astrocytic A20 on the expression of proinflammatory genes in the spinal cord during EAE, quantitative real-time PCR for cytokine and chemokine mRNA transcripts was performed on spinal cord tissue at days 15 and 22 p.i., respectively. Already at day 15 p.i., GFAP-Cre A20$^{fl/fl}$ mice had significantly increased transcription of IFN-γ, TNF, IL-6, CXCL1, and CCL2 mRNA (Fig. 4a–h). At day 22 p.i., TNF and CXCL10 mRNA were still significantly elevated in GFAP-Cre A20$^{fl/fl}$ mice as compared to control mice (Fig. 4a–h). The significantly higher levels of chemoattractant IL-6, CXCL1, CCL2, and CXCL10 mRNA in spinal cords of GFAP-Cre A20$^{fl/fl}$ mice during EAE implied that the more severe EAE in GFAP-Cre A20$^{fl/fl}$ mice might be attributed to the enhanced chemokine production by A20-deficient astrocytes.

Enhanced production of chemokines by A20-deficient astrocytes in vitro

Astrocytes have been shown as a major producer of pro-inflammatory cytokines and chemokines in the CNS during EAE upon stimulation with TNF, IFN-γ, and IL-17 [13, 59]. Therefore, we studied the regulation of chemokine production by A20 in cytokine-stimulated astrocytes in vitro. A20-deficient astrocytes expressed more CXCL10, CCL2, and CXCL1 mRNA in response to IL-17, IFN-γ, TNF, IL-17 + TNF, and IFN-γ + TNF, respectively (Fig. 5a–d). In addition, A20-deficient astrocytes expressed more IL-6 mRNA in response to IFN-γ and IFN-γ + TNF, respectively (Fig. 5c).

Although GM-CSF has been shown to play a pivotal role in EAE [44], the function of GM-CSF on astrocytes is largely unknown. A20-sufficient astrocytes expressed only low levels of CXCL10, CCL2, CXCL1, and IL-6 mRNA upon GM-CSF stimulation, but the level of all these mRNAs increased dramatically in the absence of A20 (Fig. 5). These data suggest that GM-CSF contributes to

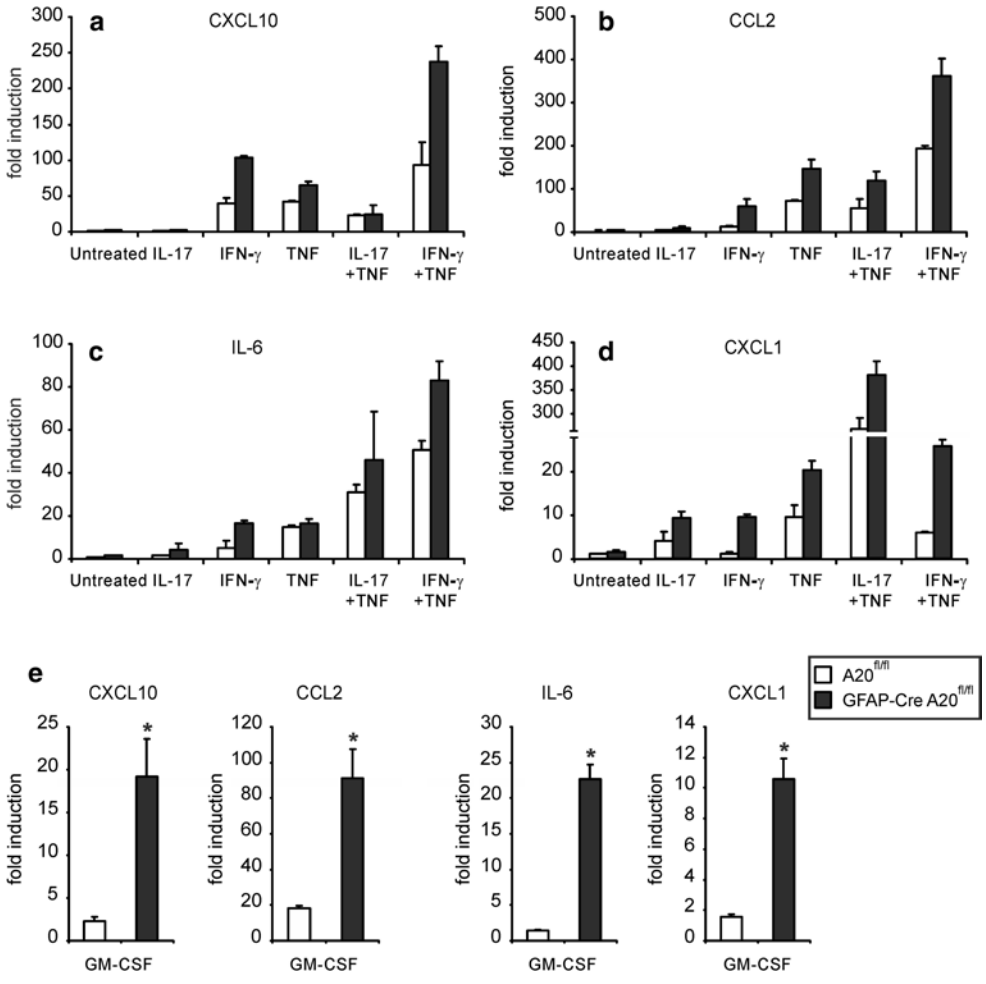

Fig. 5 Increased in vitro pro-inflammatory gene transcription in A20-deficient astrocytes. RT-PCR analysis of **a** CXCL10, **b** CCL2, **c** IL-6, and **d** CXCL1 in control ($n = 2$) and A20-deficient ($n = 2$) astrocytes left untreated or treated with IL-17 (50 ng/ml), IFN-γ (10 ng/ml), or TNF (10 ng/ml) alone or with IL-17 + TNF or IFN-γ + TNF for 16 h. Data represent the mean + SEM as relative increase over untreated control samples. **e** RT-PCR analysis of CXCL10, CCL2, IL-6, and CXCL1 in control ($n = 3$) and A20-deficient ($n = 3$) astrocytes stimulated with GM-CSF (20 ng/ml) for 16 h. Data represent the mean + SEM as relative increase over untreated control samples (*$p < 0.05$)

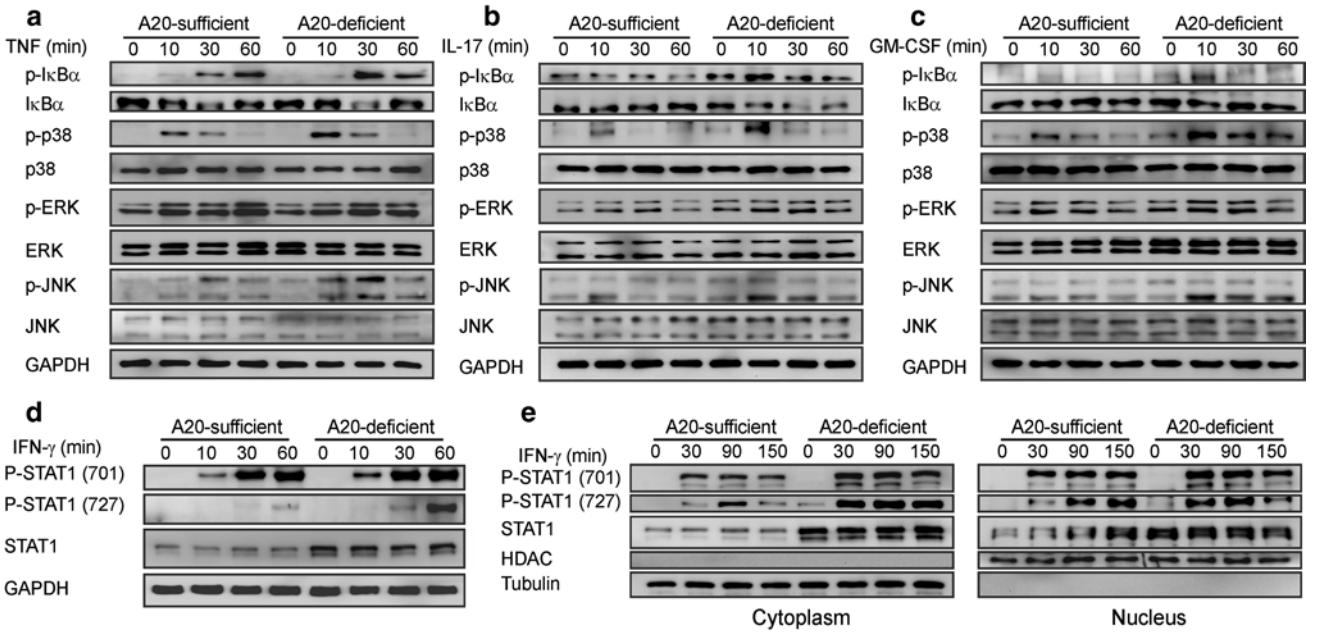

Fig. 6 A20 negatively regulates multiple signaling pathways in astrocytes. Western blot of whole cell lysates stimulated for the indicated time points with **a** TNF (10 ng/ml), **b** IL-17 (50 ng/ml), **c** GM-CSF (20 ng/ml), and **d** IFN-γ (10 ng/ml). **e** Western blot of cytoplasmic and nuclear extracts after stimulation with IFN-γ (10 ng/ml) for the indicated time points

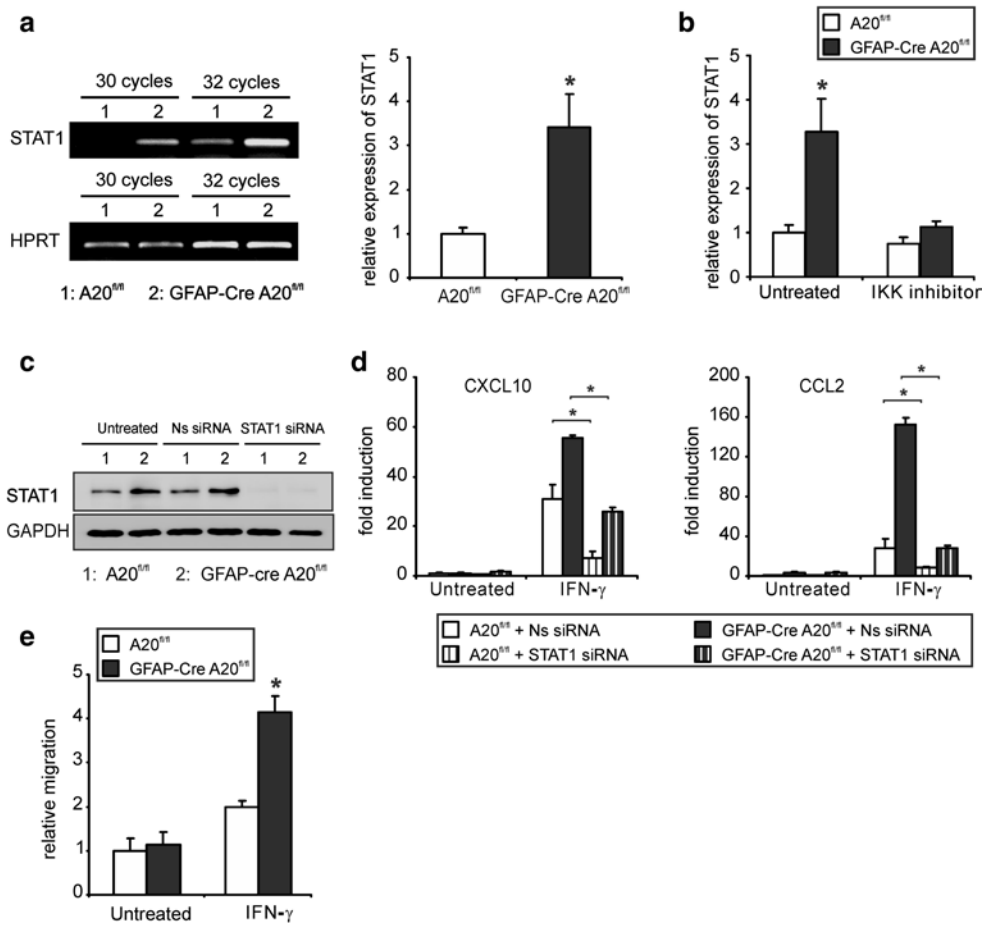

Fig. 7 A20 negatively regulates STAT1 expression on the transcriptional level in a NF-κB-dependent fashion. **a** RT-PCR analysis of STAT1 mRNA expression in cultured astrocytes derived from GFAP-Cre A20$^{fl/fl}$ and A20$^{fl/fl}$ mice (*left*). The *right panel* shows the relative quantification of STAT1 normalized to HPRT (mean + SEM $*p < 0.05$). **b** RT-PCR analysis for the STAT1 mRNA expression after IKK inhibitor (1 μM) treatment for 48 h (mean + SEM $*p < 0.05$). **c** Astrocytes derived from GFAP-Cre A20$^{fl/fl}$ and A20$^{fl/fl}$ mice were transfected with siRNA targeting STAT1 or nonsense (Ns) siRNA. Sixty hours later, WB analysis was performed on total cell lysates for STAT1 and GAPDH. **d** Sixty hours after siRNA transfection, astrocytes were left untreated or treated with IFN-γ (10 ng/ml) for 16 h. CXCL10 and CCL2 mRNA levels were determined by RT-PCR. Data represent the mean + SEM as relative increase over untreated control samples ($*p < 0.05$). **e** Purified CD4$^+$ T cells were placed into the upper part of transwell chambers with untreated or IFN-γ-conditioned medium (48 h stimulation) of cultured astrocytes isolated from GFAP-Cre A20$^{fl/fl}$ and A20$^{fl/fl}$ mice in the lower part. After 2 h of incubation, migrated T cells in the lower chambers were counted. T cell migration was calculated as relative increase over untreated controls (mean + SEM $*p < 0.05$)

the aggravated EAE in GFAP-Cre A20$^{fl/fl}$ mice at least partially by inducing chemokine production in astrocytes.

Since (i) astrocyte loss is found in the center of the demyelinated lesions in patients suffering from acute MS [43], (ii) astrocyte survival is important for the control of EAE [20, 54], and (iii) A20 can regulate apoptosis [28, 50, 55], we investigated whether the exacerbated EAE in GFAP-Cre A20$^{fl/fl}$ mice was due to enhanced astrocyte apoptosis. A20-deficient astrocytes stimulated in vitro with increasing concentrations of TNF did not undergo enhanced apoptosis as compared to A20-sufficient astrocytes (Online Resource 4) suggesting that A20 does not critically regulate apoptosis of astrocytes in EAE. Taken together, these results show that in response to proinflammatory cytokines produced by encephalitogenic T cells, A20-deficient astrocytes in GFAP-Cre A20$^{fl/fl}$ mice exhibited an elevated production of chemoattractant cytokines and chemokines, which was also observed in vivo (Fig. 4) and paralleled by increased recruitment of encephalitogenic CD4$^+$ T cells and more severe EAE.

A20 negatively regulates NF-κB, MAP kinase, and STAT1 pathways induced by fingerprint cytokines of autoreactive T cells

To understand how A20 suppresses chemokine production, we studied signaling pathways induced by TNF, IL-17, IFN-γ, and GM-CSF. Consistent with previous reports of

A20 as a negative regulator of the canonical NF-κB pathway [47] and that NF-κB pathway is activated in response to TNF, IL-17, and GM-CSF [7, 37], enhanced phosphorylation of IκBα was detected in A20-deficient astrocytes in response to all three cytokines (Fig. 6a–c). In addition, A20 deficiency also enhanced p38 and JNK phosphorylation upon stimulation with TNF, IL-17, and GM-CSF (Fig. 6a–c).

A20-deficient astrocytes produced significantly more chemokines in response to IFN-γ (Fig. 5) implying that A20 might also negatively regulate IFN-γ-induced signaling. Although phosphorylation of STAT1 at tyrosine 701 was only slightly increased in the absence of A20, phosphorylation of serine 727 was dramatically increased in A20-deficient astrocytes (Fig. 6d). An analysis of cytosolic and nuclear extracts of IFN-γ-stimulated astrocytes showed that the increased phosphorylation of serine 727 occurred in both cytoplasm and nucleus (Fig. 6e). Strikingly, the protein level of STAT1 was also increased in A20-deficient astrocytes (Fig. 6d, e).

A20 inhibits IFN-γ-induced STAT1-dependent chemokine production and T cell migration

The increased STAT1 protein levels of A20-deficient astrocytes were likely caused by an elevated STAT1 mRNA production as compared to A20-sufficient astrocytes (Fig. 7a). Interestingly, inhibition of NF-κB abolished the upregulated STAT1 mRNA production of A20-deficient astrocytes indicating that A20 indirectly modulated STAT1 function via controlling NF-κB activation (Fig. 7b). Knockdown of STAT-1 by siRNA (Fig. 7c) revealed that in IFN-γ-stimulated astrocytes the increased CXCL10 and CCL2 mRNA production was largely dependent on STAT1 (Fig. 7d). To rule out the possibility that STAT1 protein level was increased due to a genotoxic effect of the GFAP-Cre transgene, we studied the correlation between STAT1 expression and A20 expression by RNA interference (RNAi). Compared with control siRNA, A20 knockdown significantly enhanced expression of STAT1 (Online Resource 5) confirming that A20 negatively regulates the protein level of STAT1.

Since A20 strongly suppressed IFN-γ-induced STAT1-dependent chemokine production of astrocytes, we next studied the impact of A20 on astrocyte-induced T cell migration. In accordance with the in vitro chemokine production data, IFN-γ-conditioned medium of A20-deficient astrocytes induced recruitment of an increased number of $CD4^+$ T cells as demonstrated by an in vitro $CD4^+$ T cell migration assay (Fig. 7e).

Based on these findings, we conclude that A20 prevents the hyperactivation of multiple signaling pathways in astrocytes in response to cytokines produced by autoimmune T cells. Therefore, A20 suppresses the production of chemoattractant cytokines and chemokines by astrocytes, resulting in diminished recruitment of inflammatory leukocytes to the CNS and amelioration of EAE.

Discussion

The present study demonstrates that targeted deletion of A20 in neuroectodermal cells increased severity of the autoimmune demyelinating disease EAE. Consistently, previous reports showed that blocking NF-κB in neuroectodermal cells by deleting NEMO, IKK2, and Act1, respectively, ameliorated EAE [23, 52]. Although these reports point to an important function of astrocytic NF-κB in EAE, direct in vivo evidence using astrocyte-specific gene-deficient mice was still missing. Here, we extend these findings and newly show that A20 deletion in astrocytes, but not in neurons, caused an aggravated EAE by augmenting NF-κB and STAT1 activity.

Chemokine production of astrocytes is important in the effector stage of EAE that is associated with clinical disease onset [38, 59]. After priming in lymph nodes, antigen-specific T cells traffic through the choroid plexus to the subarachnoid space (Wave 1) where they are reactivated by meningeal APCs [14, 24, 45]. Consequently, T cells expand and produce inflammatory cytokines, which stimulate adjacent CNS resident cells, mainly astrocytes, to produce leukocyte-recruiting chemokines and cytokines, leading to the further recruitment of leukocytes into the CNS (Wave 2). We observed that IL-17, IFN-γ, TNF, and GM-CSF, which are signature cytokines of encephalitogenic T cells, induced significantly higher levels of CXCL1, CXCL10, CCL2, and IL-6 in A20-deficient astrocytes in vitro. In line with this, increased CXCL1, CXCL10, CCL2, and IL-6 mRNA was also detected in spinal cords of Nestin-Cre and GFAP-Cre $A20^{fl/fl}$ mice, respectively, as compared to control mice, suggesting that astrocytic A20 ameliorates EAE by inhibiting the progression of Wave 1 to Wave 2. A20 plays divergent roles in regulating apoptosis in different cell types [28, 50, 55] and astrocyte survival is critical for EAE suppression [20, 54]. In contrast, we did not obtain any evidence that A20 deficiency rendered astrocytes more sensitive to apoptosis. Thus, the more severe EAE of Nestin-Cre and GFAP-Cre $A20^{fl/fl}$ mice was not due to the enhanced apoptosis of astrocytes.

TNF, IL-17, and GM-CSF are produced by Th1 cells, Th17 cells, and GM-CSF-producing $CD4^+$ T cells, respectively, and all of them can activate the NF-κB pathway [7, 37], which drives chemokine and cytokine production in astrocytes [5, 52]. In the absence of A20, activation of NF-κB was enhanced in astrocytes upon stimulation with IL-17, TNF, and GM-CSF, respectively, explaining

the increased expression of leukocyte attracting genes in A20-deficient astrocytes. Besides, A20 also inhibited activation of p38 and JNK pathway illustrating that the inhibitory function of A20 was not restricted to NF-κB.

We repeatedly observed that IFN-γ induced a dramatic increase in chemokine production in A20-deficient astrocytes implying that A20 might interfere with IFN-γ-mediated signaling. IFN-γ-mediated STAT1 activation was stronger in the absence of A20 as shown by increased STAT1 phosphorylation at serine 727, which is required for the full activation of STAT1 [11, 53]. Interestingly, STAT1 protein was also increased in unstimulated and IFN-γ-stimulated A20-deficient astrocytes, which was caused by an enhanced NF-κB-dependent STAT1 mRNA production in the absence of A20, showing that STAT1 signaling pathway was also negatively regulated by A20. Therefore, it is possible that NF-κB-activating cytokines such as IL17, TNF, and GM-CSF induce increased chemokine production in A20-deficient astrocytes by cooperation with IFN-γ-dependent STAT1 activation. In fact, treatment with TNF + IFN-γ resulted in an augmented production of chemokines and cytokines in A20-deficient astrocytes.

STAT1 protein levels can be regulated by K48 ubiquitin-dependent proteasomal degradation that is induced by the E3 ligase Smurf1 [58]. As an ubiquitin E3 ligase, A20 is involved in the proteasomal degradation of several signaling molecules including RIP1 [57]. However, no direct interaction between A20 and STAT1 was detected by immunoprecipitation (data not shown) ruling out the possibility that A20 promoted the degradation of STAT1 by K48-ubiquitination or inhibited its function by K63-deubiquitination. Instead, we observed higher STAT1 mRNA expression in A20-deficient astrocytes than in control cells, indicating that the increased STAT1 protein level in A20-deficient astrocytes should be attributed to increased production but not to reduced degradation. Although numerous reports mentioned phosphorylation of STAT1, barely any of them elucidated STAT1 production. We showed that A20 negatively regulated STAT1 production indirectly by inhibiting the NF-κB signaling cascade that is responsible for STAT1 mRNA synthesis. Our novel observation that A20 inhibited STAT1 at both expression and phosphorylation levels explains why IFN-γ-stimulated A20-deficient astrocytes produced more chemokines as compared to A20-sufficient astrocytes. The enhanced migration of wildtype $CD4^+$ T cells in response to IFN-γ conditioned medium of A20-deficient astrocytes also provided direct evidence that the enhanced production of chemoattractant molecules by A20-deficient astrocytes induced $CD4^+$ T cell recruitment.

Recent genome-wide association study (GWAS) identified OLIG3/TNFAIP3 as a susceptibility locus for MS [10, 22]. In addition, TNFAIP3 expression was found to be tightly correlated with clinical features of MS [16]. Compared with healthy controls, a lower mRNA expression of TNFAIP3 was observed in untreated patients with MS and its baseline levels were lower in patients with a more malignant disease course than in patients with a more benign course. Accordingly, treatment of MS patients with glatiramer acetate reverted TNFAIP3 expression to levels displayed by healthy controls. A recent study showed that SNPs in the OLIG3/TNFAIP3 gene correlated significantly with increased cerebrospinal fluid (CSF) levels of the chemokine CXCL13, a prognostic marker for MS [30]. Given that our study shows that astrocytic A20 suppresses EAE by inhibiting chemokine production in astrocytes, it therefore provides a biological rationale for the clinical observation that SNPs in or close to TNFAIP3 gene influence the development of MS. Thus, therapeutical augmentation of A20 in astrocytes might be beneficial for the treatment of MS.

Acknowledgments The authors thank Elena Fischer, Nadja Schlüter, and Annette Sohnekind for technical assistance. This work was supported by grants of the Deutsche Forschungsgemeinschaft (GRK 1167 to DS; SFB 854/TP5 to DS and MN).

References

1. Anderton SM, Liblau RS (2008) Regulatory T cells in the control of inflammatory demyelinating diseases of the central nervous system. Curr Opin Neurol 21(3):248–254
2. Bajenaru ML, Zhu Y, Hedrick NM, Donahoe J, Parada LF, Gutmann DH (2002) Astrocyte-specific inactivation of the neurofibromatosis 1 gene (NF1) is insufficient for astrocytoma formation. Mol Cell Biol 22(14):5100–5113
3. Baxter AG (2007) The origin and application of experimental autoimmune encephalomyelitis. Nat Rev Immunol 7(11):904–912
4. Brambilla R, Persaud T, Hu X, Karmally S, Shestopalov VI, Dvoriantchikova G, Ivanov D, Nathanson L, Barnum SR, Bethea JR (2009) Transgenic inhibition of astroglial NF-kappa B improves functional outcome in experimental autoimmune encephalomyelitis by suppressing chronic central nervous system inflammation. J Immunol 182(5):2628–2640
5. Brück W, Pförtner R, Pham T, Zhang J, Hayardeny L, Piryatinsky V, Hanisch UK, Regen T, van Rossum D, Brakelmann L, Hagemeier K, Kuhlmann T, Stadelmann C, John GR, Kramann N, Wegner C (2012) Reduced astrocytic NF-kappaB activation by laquinimod protects from cuprizone-induced demyelination. Acta Neuropathol 124(3):411–424
6. Brüstle A, Brenner D, Knobbe CB, Lang PA, Virtanen C, Hershenfield BM, Reardon C, Lacher SM, Ruland J, Ohashi PS, Mak TW (2012) The NF-kappaB regulator MALT1 determines the encephalitogenic potential of Th17 cells. J Clin Invest 122(12):4698–4709
7. Bulek K, Liu C, Swaidani S, Wang L, Page RC, Gulen MF, Herjan T, Abbadi A, Qian W, Sun D, Lauer M, Hascall V, Misra S, Chance MR, Aronica M, Hamilton T, Li X (2011) The inducible kinase IKKi is required for IL-17-dependent signaling associated with neutrophilia and pulmonary inflammation. Nat Immunol 12(9):844–852

8. Chu Y, Vahl JC, Kumar D, Heger K, Bertossi A, Wojtowicz E, Soberon V, Schenten D, Mack B, Reutelshöfer M, Beyaert R, Amann K, van Loo G, Schmidt-Supprian M (2011) B cells lacking the tumor suppressor TNFAIP3/A20 display impaired differentiation and hyperactivation and cause inflammation and autoimmunity in aged mice. Blood 117(7):2227–2236
9. Codarri L, Gyülveszi G, Tosevski V, Hesske L, Fontana A, Magnenat L, Suter T, Becher B (2011) RORgammat drives production of the cytokine GM-CSF in helper T cells, which is essential for the effector phase of autoimmune neuroinflammation. Nat Immunol 12(6):560–567
10. De Jager PL, Jia X, Wang J, de Bakker PI, Ottoboni L, Aggarwal NT, Piccio L, Raychaudhuri S, Tran D, Aubin C, Briskin R, Romano S, Baranzini SE, McCauley JL, Pericak-Vance MA, Haines JL, Gibson RA, Naeglin Y, Uitdehaag B, Matthews PM, Kappos L, Polman C, McArdle WL, Strachan DP, Evans D, Cross AH, Daly MJ, Compston A, Sawcer SJ, Weiner HL, Hauser SL, Hafler DA, Oksenberg JR (2009) Meta-analysis of genome scans and replication identify CD6, IRF8 and TNFRSF1A as new multiple sclerosis susceptibility loci. Nat Genet 41(7):776–782
11. Decker T, Kovarik P (2000) Serine phosphorylation of STATs. Oncogene 19(21):2628–2637
12. Domingues HS, Mues M, Lassmann H, Wekerle H, Krishnamoorthy G (2010) Functional and pathogenic differences of Th1 and Th17 cells in experimental autoimmune encephalomyelitis. PLoS One 5(11):e15531
13. Dong Y, Benveniste EN (2001) Immune function of astrocytes. Glia 36(2):180–190
14. Engelhardt B, Sorokin L (2009) The blood–brain and the blood–cerebrospinal fluid barriers: function and dysfunction. Semin Immunopathol 31(4):497–511
15. Fung EY, Smyth DJ, Howson JM, Cooper JD, Walker NM, Stevens H, Wicker LS, Todd JA (2009) Analysis of 17 autoimmune disease-associated variants in type 1 diabetes identifies 6q23/TNFAIP3 as a susceptibility locus. Genes Immun 10(2):188–191
16. Gilli F, Navone ND, Perga S, Marnetto F, Caldano M, Capobianco M, Pulizzi A, Malucchi S, Bertolotto A (2011) Loss of braking signals during inflammation: a factor affecting the development and disease course of multiple sclerosis. Arch Neurol 68(7):879–888
17. Graus-Porta D, Blaess S, Senften M, Littlewood-Evans A, Damsky C, Huang Z, Orban P, Klein R, Schittny JC, Müller U (2001) Beta1-class integrins regulate the development of laminae and folia in the cerebral and cerebellar cortex. Neuron 31(3):367–379
18. Hammer GE, Turer EE, Taylor KE, Fang CJ, Advincula R, Oshima S, Barrera J, Huang EJ, Hou B, Malynn BA, Reizis B, DeFranco A, Criswell LA, Nakamura MC, Ma A (2011) Expression of A20 by dendritic cells preserves immune homeostasis and prevents colitis and spondyloarthritis. Nat Immunol 12(12):1184–1193
19. Händel U, Brunn A, Drögemüller K, Müller W, Deckert M, Schlüter D (2012) Neuronal gp130 expression is crucial to prevent neuronal loss, hyperinflammation, and lethal course of murine Toxoplasma encephalitis. Am J Pathol 181(1):163–173
20. Haroon F, Drögemüller K, Händel U, Brunn A, Reinhold D, Nishanth G, Mueller W, Trautwein C, Ernst M, Deckert M, Schlüter D (2011) Gp130-dependent astrocytic survival is critical for the control of autoimmune central nervous system inflammation. J Immunol 186(11):6521–6531
21. Hövelmeyer N, Reissig S, Xuan NT, Adams-Quack P, Lukas D, Nikolaev A, Schlüter D, Waisman A (2011) A20 deficiency in B cells enhances B-cell proliferation and results in the development of autoantibodies. Eur J Immunol 41(3):595–601
22. International Multiple Sclerosis Genetics Consortium (IMSGC) (2010) IL12A, MPHOSPH9/CDK2AP1 and RGS1 are novel multiple sclerosis susceptibility loci. Genes Immun 11(5):397–405
23. Kang Z, Altuntas CZ, Gulen MF, Liu C, Giltiay N, Qin H, Liu L, Qian W, Ransohoff RM, Bergmann C, Stohlman S, Tuohy VK, Li X (2010) Astrocyte-restricted ablation of interleukin-17-induced Act1-mediated signaling ameliorates autoimmune encephalomyelitis. Immunity 32(3):414–425
24. Kebir H, Kreymborg K, Ifergan I, Dodelet-Devillers A, Cayrol R, Bernard M, Giuliani F, Arbour N, Becher B, Prat A (2007) Human TH17 lymphocytes promote blood–brain barrier disruption and central nervous system inflammation. Nat Med 13(10):1173–1175
25. Kool M, van Loo G, Waelput W, De Prijck S, Muskens F, Sze M, van Praet J, Branco-Madeira F, Janssens S, Reizis B, Elewaut D, Beyaert R, Hammad H, Lambrecht BN (2011) The ubiquitin-editing protein A20 prevents dendritic cell activation, recognition of apoptotic cells, and systemic autoimmunity. Immunity 35(1):82–96
26. Langrish CL, Chen Y, Blumenschein WM, Mattson J, Basham B, Sedgwick JD, McClanahan T, Kastelein RA, Cua DJ (2005) IL-23 drives a pathogenic T cell population that induces autoimmune inflammation. J Exp Med 201(2):233–240
27. Le DG, Kular L, Nicot AB, Calmel C, Melik-Parsadaniantz S, Kitabgi P, Laurent M, Martinerie C (2010) NOV/CCN3 upregulates CCL2 and CXCL1 expression in astrocytes through beta1 and beta5 integrins. Glia 58(12):1510–1521
28. Lee EG, Boone DL, Chai S, Libby SL, Chien M, Lodolce JP, Ma A (2000) Failure to regulate TNF-induced NF-kappaB and cell death responses in A20-deficient mice. Science 289(5488):2350–2354
29. Lees JR, Golumbek PT, Sim J, Dorsey D, Russell JH (2008) Regional CNS responses to IFN-gamma determine lesion localization patterns during EAE pathogenesis. J Exp Med 205(11):2633–2642
30. Linden M, Khademi M, Lima Bomfim I, Piehl F, Jagodic M, Kockum I, Olsson T (2013) Multiple sclerosis risk genotypes correlate with an elevated cerebrospinal fluid level of the suggested prognostic marker CXCL13. Mult Scler 19(7):863–870
31. Liu Y, Teige I, Birnir B, Issazadeh-Navikas S (2006) Neuron-mediated generation of regulatory T cells from encephalitogenic T cells suppresses EAE. Nat Med 12(5):518–525
32. Livak KJ, Schmittgen TD (2001) Analysis of relative gene expression data using real-time quantitative PCR and the 2(−Delta Delta C(T)) method. Methods 25(4):402–408
33. Ma A, Malynn BA (2012) A20: linking a complex regulator of ubiquitylation to immunity and human disease. Nat Rev Immunol 12(11):774–785
34. Matmati M, Jacques P, Maelfait J, Verheugen E, Kool M, Sze M, Geboes L, Louagie E, Mc Guire C, Vereecke L, Chu Y, Boon L, Staelens S, Matthys P, Lambrecht BN, Schmidt-Supprian M, Pasparakis M, Elewaut D, Beyaert R, van Loo G (2011) A20 (TNFAIP3) deficiency in myeloid cells triggers erosive polyarthritis resembling rheumatoid arthritis. Nat Genet 43(9):908–912
35. McFarland HF, Martin R (2007) Multiple sclerosis: a complicated picture of autoimmunity. Nat Immunol 8(9):913–919
36. McGeachy MJ, Stephens LA, Anderton SM (2005) Natural recovery and protection from autoimmune encephalomyelitis: contribution of CD4+CD25+ regulatory cells within the central nervous system. J Immunol 175(5):3025–3032
37. Meads MB, Li ZW, Dalton WS (2010) A novel TNF receptor-associated factor 6 binding domain mediates NF-kappa B signaling by the common cytokine receptor beta subunit. J Immunol 185(3):1606–1615
38. Miljkovic D, Timotijevic G, Mostarica SM (2011) Astrocytes in the tempest of multiple sclerosis. FEBS Lett 585(23):3781–3788

39. Musone SL, Taylor KE, Lu TT, Nititham J, Ferreira RC, Ortmann W, Shifrin N, Petri MA, Kamboh MI, Manzi S, Seldin MF, Gregersen PK, Behrens TW, Ma A, Kwok PY, Criswell LA (2008) Multiple polymorphisms in the TNFAIP3 region are independently associated with systemic lupus erythematosus. Nat Genet 40(9):1062–1064
40. Musone SL, Taylor KE, Nititham J, Chu C, Poon A, Liao W, Lam ET, Ma A, Kwok PY, Criswell LA (2011) Sequencing of TNFAIP3 and association of variants with multiple autoimmune diseases. Genes Immun 12(3):176–182
41. Nair A, Frederick TJ, Miller SD (2008) Astrocytes in multiple sclerosis: a product of their environment. Cell Mol Life Sci 65(17):2702–2720
42. Nair RP, Duffin KC, Helms C, Ding J, Stuart PE, Goldgar D, Gudjonsson JE, Li Y, Tejasvi T, Feng BJ, Ruether A, Schreiber S, Weichenthal M, Gladman D, Rahman P, Schrodi SJ, Prahalad S, Guthery SL, Fischer J, Liao W, Kwok PY, Menter A, Lathrop GM, Wise CA, Begovich AB, Voorhees JJ, Elder JT, Krueger GG, Bowcock AM, Abecasis GR (2009) Genome-wide scan reveals association of psoriasis with IL-23 and NF-kappaB pathways. Nat Genet 41(2):199–204
43. Ozawa K, Suchanek G, Breitschopf H, Bruck W, Budka H, Jellinger K, Lassmann H (1994) Patterns of oligodendroglia pathology in multiple sclerosis. Brain 117(Pt 6):1311–1322
44. Petermann F, Korn T (2011) Cytokines and effector T cell subsets causing autoimmune CNS disease. FEBS Lett 585(23):3747–3757
45. Reboldi A, Coisne C, Baumjohann D, Benvenuto F, Bottinelli D, Lira S, Uccelli A, Lanzavecchia A, Engelhardt B, Sallusto F (2009) C–C chemokine receptor 6-regulated entry of TH-17 cells into the CNS through the choroid plexus is required for the initiation of EAE. Nat Immunol 10(5):514–523
46. Shembade N, Ma A, Harhaj EW (2010) Inhibition of NF-kappaB signaling by A20 through disruption of ubiquitin enzyme complexes. Science 327(5969):1135–1139
47. Skaug B, Chen J, Du F, He J, Ma A, Chen ZJ (2011) Direct, noncatalytic mechanism of IKK inhibition by A20. Mol Cell 44(4):559–571
48. Sofroniew MV, Vinters HV (2010) Astrocytes: biology and pathology. Acta Neuropathol 119(1):7–35
49. Stromnes IM, Cerretti LM, Liggitt D, Harris RA, Goverman JM (2008) Differential regulation of central nervous system autoimmunity by T(H)1 and T(H)17 cells. Nat Med 14(3):337–342
50. Tavares RM, Turer EE, Liu CL, Advincula R, Scapini P, Rhee L, Barrera J, Lowell CA, Utz PJ, Malynn BA, Ma A (2010) The ubiquitin modifying enzyme A20 restricts B cell survival and prevents autoimmunity. Immunity 33(2):181–191
51. Tronche F, Kellendonk C, Kretz O, Gass P, Anlag K, Orban PC, Bock R, Klein R, Schutz G (1999) Disruption of the glucocorticoid receptor gene in the nervous system results in reduced anxiety. Nat Genet 23(1):99–103
52. van Loo G, De Lorenzi R, Schmidt H, Huth M, Mildner A, Schmidt-Supprian M, Lassmann H, Prinz MR, Pasparakis M (2006) Inhibition of transcription factor NF-kappaB in the central nervous system ameliorates autoimmune encephalomyelitis in mice. Nat Immunol 7(9):954–961
53. Varinou L, Ramsauer K, Karaghiosoff M, Kolbe T, Pfeffer K, Müller M, Decker T (2003) Phosphorylation of the Stat1 transactivation domain is required for full-fledged IFN-gamma-dependent innate immunity. Immunity 19(6):793–802
54. Voskuhl RR, Peterson RS, Song B, Ao Y, Morales LB, Tiwari-Woodruff S, Sofroniew MV (2009) Reactive astrocytes form scar-like perivascular barriers to leukocytes during adaptive immune inflammation of the CNS. J Neurosci 29(37):11511–11522
55. Vucic D, Dixit VM, Wertz IE (2011) Ubiquitylation in apoptosis: a post-translational modification at the edge of life and death. Nat Rev Mol Cell Biol 12(7):439–452
56. Wang X, Haroon F, Karray S, Martina D, Schlüter D (2013) Astrocytic Fas ligand expression is required to induce T-cell apoptosis and recovery from experimental autoimmune encephalomyelitis. Eur J Immunol 43(1):115–124
57. Wertz IE, O'Rourke KM, Zhou H, Eby M, Aravind L, Seshagiri S, Wu P, Wiesmann C, Baker R, Boone DL, Ma A, Koonin EV, Dixit VM (2004) De-ubiquitination and ubiquitin ligase domains of A20 downregulate NF-kappaB signalling. Nature 430(7000):694–699
58. Yuan C, Qi J, Zhao X, Gao C (2012) Smurf1 protein negatively regulates interferon-gamma signaling through promoting STAT1 protein ubiquitination and degradation. J Biol Chem 287(21):17006–17015
59. Zepp J, Wu L, Li X (2011) IL-17 receptor signaling and T helper 17-mediated autoimmune demyelinating disease. Trends Immunol 32(5):232–239
60. Zhu Y, Romero MI, Ghosh P, Ye Z, Charnay P, Rushing EJ, Marth JD, Parada LF (2001) Ablation of NF1 function in neurons induces abnormal development of cerebral cortex and reactive gliosis in the brain. Genes Dev 15(7):859–876